Desalination and Water Treatment
www.deswater.com

doi: 10.5004/dwt.2017.21650

99 (2017) 155–161
December

Optimization of polysulfone support layer for thin-film composite forward osmosis membrane

Aatif Ali Shah[a,b,†], Hyeon-gyu Choi[a,†], Seung-Eun Nam[a], Ahrumi Park[a], Pyung Soo Lee[a,b], You-In Park[a,b,*], Hosik Park[a,b,*]

[a]*Center for Membranes, Advanced Materials Division, Korea Research Institute of Chemical Technology, 141 Gajeong-ro, Yuseong-gu, Daejeon 34114, Korea, Tel. +82-42-860-7241; Fax: +82-42-860-7283; email: yipark@krict.re.kr (Y.-I. Park), Tel. +82-42-860-7510; email: hspark@krict.re.kr (H. Park)*
[b]*Department of Green Chemistry and Environmental Biotechnology, University of Science and Technology, 217 Gajeong-ro, Yuseong-gu, Daejeon 34113, Korea*

Received 27 August 2017; Accepted 28 October 2017

ABSTRACT

Polysulfone (PSf) has been applied to thin-film composite (TFC) membranes for water treatment and desalination due to its good physicochemical resistance and high affinity for polyamide. In this study, the effect of the PSf support layer synthesis conditions on TFC membrane performance was investigated in order to optimize membrane performance for forward osmosis (FO) process. Scanning electron microscopy, pure water permeability, molecular weight cut-off, and lab-scale FO tests were conducted. The polymer concentration and casting thickness of PSf support layer were critical for determining membrane structure, selectivity, and permeability. The results indicated that TFC FO membrane with PSf support layer fabricated by 15 wt% PSf polymer concentration and 100 μm casting thickness showed the best performance for FO process. The results of this study could contribute to the development of a commercial TFC FO membrane for water treatment and desalination applications.

Keywords: Forward osmosis; Polysulfone; Phase inversion; Interfacial polymerization; Thin-film composite membrane; Fabrication optimization

1. Introduction

During the last decade, forward osmosis (FO) has received academic and industrial attention for desalination as well as for water treatment, food and drug industry, and energy applications [1,2]. Key advantages of FO include its reversible fouling characteristic and no hydraulic pressure requirement. The development of draw solute such as ammonia–carbon dioxide for FO process and the invention of cellulose triacetate FO membrane have stimulated academic and industrial interest in the FO process [3,4]. Much research has been conducted to establish field applications of FO [1,2,5]. However, despite vigorous efforts, huddles will remain for establishing a stand-alone FO process.

The key challenges in the FO process for the real field application are (1) development of draw solutes that allows high osmotic pressure and easy recovery with low energy consumption and (2) fabrication of FO membranes that shows excellent permeability and selectivity [6]. The important draw solute characteristics include osmotic pressure, water solubility, viscosity, toxicity, and diffusivity; therefore, various inorganic compounds [7–9] and organic compounds [10–14] have been studied. Different technical methods, such as heating, air stripping, distillation, and other membrane processes, have also been tried for draw solute regeneration [9,15–17].

Another important aspect of FO process is the development of highly efficient membranes. In 2000s, cellulose

* Corresponding author.

† These authors equally contributed to this work.

acetate-based polymers, which were widely used for asymmetric membrane fabrication, based on the traditional asymmetric membrane developed by Loeb and Sourirajan has been focused for FO applications [18]. The use of low acetylation cellulose acetate allowed membranes with more hydrophilic nature, while high acetylation imparted a high degree of crystallinity under heating [19]. This polymer was therefore appropriate for use in osmotically driven membranes. A wetting process decreased the internal concentration polarization (ICP) and increased the water flux [20]. Although cellulose acetate-based membranes have been widely used for FO application studies, it still has some challenges to overcome such as lower water flux, limited range to pH tolerability (pH 4–8), and concentration polarization effect.

To overcome these issues, recently thin-film composite (TFC) membranes have been actively studied for FO processes [21]. Generally, polysulfone (PSf) and polyethersulfone with an aryl-SO_2-aryl group have been utilized as porous support layers to fabricate the TFC FO membranes. These polymers showed good thermal oxidative resistance and chemical resistance to hydrolysis and industrial solvents. Their amorphous structure imparted a hydrophilic nature, which enhanced the transport of water molecules while simultaneously increasing the ICP in the osmotic process [18]. Polyamide (PA) has been used as a selective dense layer in TFC membranes since the introduction of the interfacial polymerization (IP) concept [22]. This IP phenomenon takes place between two reacting monomers (two immiscible phases) at the interface of PSf porous support [23]. The most commonly used monomer combination for FO applications is trimesoyl chloride (TMC) as an acid chloride and *m*-phenylenediamine (MPD) as an amine due to its the excellent water flux and salt rejection.

Despite vigorous academic efforts, FO membranes have not reached the real field application level yet, which implies that better membrane performance is still desired. Recent studies have shown that the permeability–selectivity trade-off correlation is a critical consideration and that permeability enhancement was especially required to maximize membrane performance [24,25]. These researchers suggested that a highly permeable support layer had a great potential to enhance membrane performance and that additional studies were required for the support layer synthesis optimization.

This study examined the effect of the structure of the TFC membrane support layer on the FO performance. PSf was selected as the support layer membrane material, and the PSf concentration for the polymer dope solution and the casting thickness for the PSf dope solution film were selected as the main fabrication factors for preparation of a permeability-enhanced support layer. The main objectives of this study were: (1) to fabricate PSf support layers using different PSf concentrations for the polymer dope solution, (2) to evaluate the permeability of these PSf support layers, (3) to fabricate TFC membranes using different PSf support layers prepared by different casting thicknesses with fixed PSf concentrations, and (4) to evaluate the FO performance of these TFC membranes to determine the roles of these fabrication factors.

2. Experimental

2.1. Materials and chemicals

PSf (MW = 52,000 Da, BASF, Germany), 1-methyl-2-pyrrolidine (NMP; anhydrous, 99%, Samchun, Korea), and polyvinylpyrrolidone (PVP; K-30, Kanto Chemical Co., Japan) were purchased for the synthesis of the PSf support layers. TMC (98%, Sigma-Aldrich, USA), MPD (Flakes 99%, Sigma-Aldrich), and Isol-C (SK Chemical, Korea) were used for formation of the PA selective layers. Polyethylene glycol (PEG; MW = 8, 20, 35, 100, 200, 300, 400, 600, 900, and 1,000 kDa, Sigma-Aldrich) was used for molecular weight cut-off (MWCO) tests of the PSf support layers. Sodium chloride (NaCl, 99%, Samchun) was used as a draw solute in the FO operation. All aqueous solutions for the experiments were prepared using deionized (DI) water from a DI water purification system (RiOs™ Essential, Millipore, USA) that produced with a resistivity of 18.2 mΩ cm. A film applicator (YBA-5, Yoshimitsu, Japan) was purchased for casting the PSf support layers.

2.2. Polysulfone support layer synthesis

The PSf support layers were synthesized by a phase inversion method. The PSf polymer and PVP were dissolved in the NMP solvent for 12 h with gentle stirring. Different ratios of PSf to total polymer solution were used to investigate the effect of polymer concentration on membrane permeability (Table 1). The polymer solution was placed in a vacuum oven (OV-11, Jeio Tech, Korea) overnight at room temperature to remove air bubbles. That solution was then cast with a film applicator with 100, 150, and 200 μm thickness onto woven polyethylene terephthalate (PET) fabric positioned on a glass plate (Fig. 1). The resulting casted PSf support layer was placed into a coagulation bath for 30 min, using DI water as the non-solvent. The synthesized PSf support layer was rinsed with DI water and stored in DI water until lab-scale testing or PA selective layer formation.

2.3. PA selective layer formation

The PA selective layer on the PSf support layer was formed by an IP method. The synthesized PSf support layer was mounted in a bespoke acrylic frame and 100 mL of 3 wt% aqueous MPD solution was poured onto the surface of the PSf support layer and left for 2 min. The residual MPD solution was then removed with a rubber roller. The MPD-saturated PSf support layer was then immersed in 0.15 wt% TMC solution in Isol-C for 1 min (Fig. 1). The membrane was cured in

Table 1
The chemical composition of the PSf polymer solutions used to fabricate PSf support layers

Membrane ID	PSf (w/w %)	NMP (w/w %)	PVP (w/w %)
PSf 13	13	85	2
PSf 15	15	83	2
PSf 18	18	80	2

PSf, polysulfone; NMP, 1-methyl-2-pyrrolidine; PVP, polyvinylpyrrolidone.

an oven at 60°C for 10 min and then stored in DI water until lab-scale test.

2.4. Membrane characterization and lab-scale test

The surface and cross-sectional morphologies of the PSf support layers and the TFC membranes were observed by field emission scanning electron microscope (Mira 3, Tescan, Czech Republic). The actual membrane thickness was determined from scanning electron microscopic (SEM) images.

A lab-scale cross-flow membrane test unit was used for the pure water permeability test and MWCO test. For these tests, the temperature in the unit was maintained at 25°C with an open heating bath circulator (CW-20G, Jeio Tech). The test unit used a gear type pump (Hydra-Cell Pump, Wanner Engineering Inc., USA) and the effective membrane area was 3.90 cm^2. The transmembrane pressure was increased up to 8 bar and cross-flow rate was kept constant at 1,000 mL/min. For the MWCO test, a PEG rejection rate of the PSf support layer was measured in the lab-scale membrane operation. The feed solution was 100 ppm PEG of the desired molecular weight and the transmembrane pressure was maintained at 1 bar. The concentration of PEG solution was analyzed with a total organic carbon analyzer (TOC-L, Dong-il Shimadzu, Korea). All membrane samples were stabilized for 1 h with DI water at a transmembrane pressure of 15 bar.

The lab-scale cross-flow FO membrane test unit was used for water flux and reverse solute flux (RSF) measurements. 1 M NaCl aqueous solution was used as the draw solution and DI water was used as the feed solution. The temperatures of the draw and the feed solutions were controlled at 25°C with a heating bath circulator (CW-20G, Lab Companion, Korea). The solutions were circulated using a gear pump (EW-74013-45, Cole-Parmer Instrument, USA) with a 1,000 mL/min cross-flow rate and the effective membrane area was 3.90 cm^2. The water permeation flux was obtained by calculating in which the permeated volume rate divided by the effective membrane area:

$$J_W\left(\mathrm{L/m^2h,LMH}\right)=\frac{V_{F0}-V_F}{A_m t}$$

where J_W is the water permeated flux, V_{F0} is the initial volume of the feed solution, V_F is the final volume of the feed solution after operation time t, and A_m is the effective membrane area. The RSF is obtained by calculating the NaCl concentration of the feed solution from its electrical conductivity measurements obtained with a conductivity meter (CON 11 Economy Meter, Oakton Eutech Instruments, Malaysia) using the following equation:

$$J_S\left(\mathrm{g/mol\cdot h,gMH}\right)=\frac{c_F-c_0}{A_m t}$$

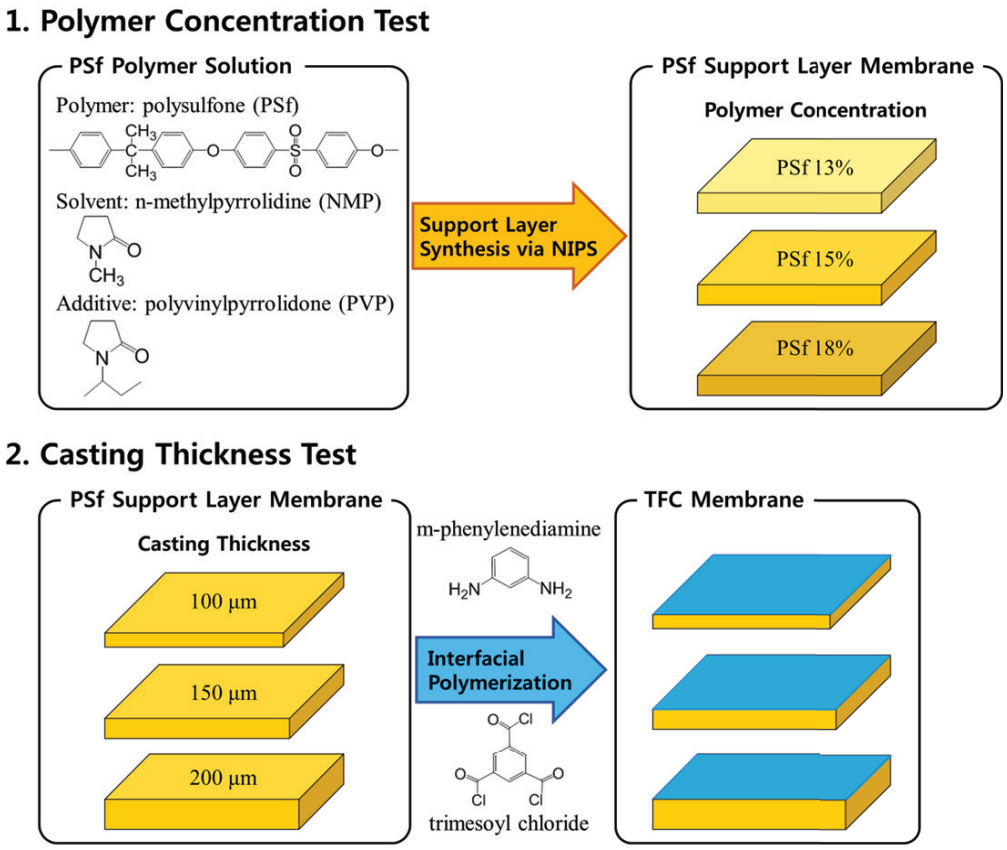

Fig. 1. Conceptual images for the synthesis of polysulfone (PSf) support layers with different polymer concentrations and casting thicknesses for preparation of thin-film composite (TFC) membranes.

where J_S is the RSF, c_0 is the initial NaCl concentration of the feed solution, c_F is the final NaCl concentration of the feed solution after operation time t, and A_m is the effective membrane area. Membrane selectivity was obtained to evaluate the membrane permselectivity by calculating the RSF divided by the water permeated flux.

$$\text{Selectivity}\left(\text{g/L}\right) = \frac{J_S}{J_W}$$

3. Results and discussion

3.1. Effect of polymer concentration

The support layers with concentrations of 13–18 wt% of polymer (PSf), denoted as PSf 13, PSf 15, and PSf 18, were prepared to investigate the effect of polymer concentration on the structure and performance of PSf support layers. Fig. 2 shows SEM cross-sectional and surface images of the PSf support layers with the given PSf concentrations. All PSf support layers exhibited asymmetric and surface-porous structures. The PSf 13 had more open pores and a higher porosity when compared with PSf 15 and PSf 18. Increases in the PSf concentration of the support layer resulted in a denser top surface and fewer and smaller open pores, as shown in Figs. 2(a)–(c).

The cross-sectional views of the PSf support layers revealed that they all had an asymmetric finger-like morphology with a dense top structure, which increased with increases in the polymer concentration in the casting solution. Penetration of the polymeric layer structure through the woven fabric was observed in the PSf 13, as shown in Fig. 2(d). For all polymer concentrations PSf supports exhibited conventional asymmetric morphology that is comprised of finger-like structure except PSf 18 which partially shows a sponge-like structure. A finger-like macrovoid was clearly observed in Figs. 2(d) and (e) for low polymer concentration (i.e., PSf 13 and PSf 15) throughout the support span, while at high polymer concentration (i.e., PSf 18) smaller macrovoids was observed in Fig. 2(f). These changes can be associated with viscosity of polymer solutions. It is accepted that, viscosity of polymer solution has significant impact on morphology of support. As with increase in polymer concentration increase in viscosity and it extraordinarily reduced the exchange rate of solvent and non-solvent all along precipitation process. At higher dope concentration, result in higher polymer concentration at reaction interface and consequently growth of less porous structure as well as sponge-like morphology was observed in Fig. 2(f) [26–28].

The MWCO test was conducted using different PEGs to investigate the surface pore sizes of the PSf support layers followed by solute rejection measurement [29,30]. Fig. 3 shows the PEG rejections and surface pore sizes for the PSf support layer membranes with different polymer concentrations. The surface pore size was obtained with a previously described calculation [31]. The MWCO and surface pore size became smaller as the PSf concentration in the casting solution increased. The PSf 13 membrane showed a maximum MWCO and pore size, whereas the PSf 18 membrane showed a minimum MWCO and pore size (MWCO: 558.8 kDa (PSf 13), 291.2 kDa (PSf 15), and 34 kDa (PSf 18); pore size: 13.64 nm (PSf 13), 10.98 nm (PSf 15), and 5.37 nm (PSf 18)). As discussed above, a lower polymer concentration created more open pores on the surface, which resulted in increased in the MWCO as shown in Fig. 3.

Fig. 4 shows the pure water permeabilities of the PSf support layers with different polymer concentrations. The permeability was measured in a range of transmembrane pressures from 0.2 to 10 bar. PSf 15 showed the highest water flux (109.48 LMH/bar), PSf 13 showed a moderate water flux

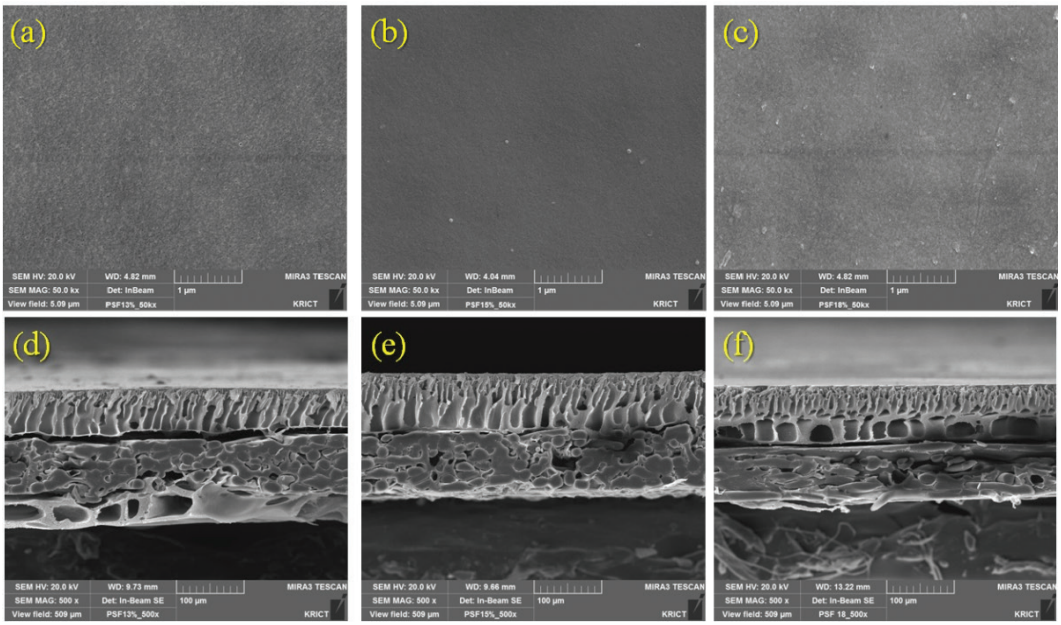

Fig. 2. Scanning electron microscopy (SEM) images of the surfaces (a)–(c) and cross-sections (d)–(f) of PSf support layers with different PSf concentrations: 13 wt% (a) and (d), 15 wt% (b) and (e), and 18 wt% (c) and (f).

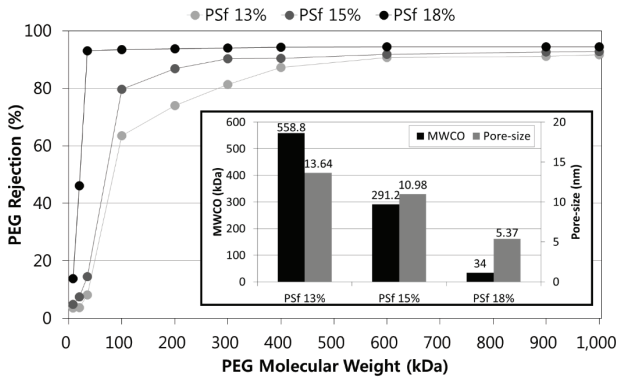

Fig. 3. Polyethylene glycol (PEG) rejections for PSf support layers with PSf 13 wt%, PSf 15 wt%, and PSf 18 wt% polymer concentration. Bottom inset shows molecular weight cut-offs (MWCOs) and surface pore sizes of the PSf support layers.

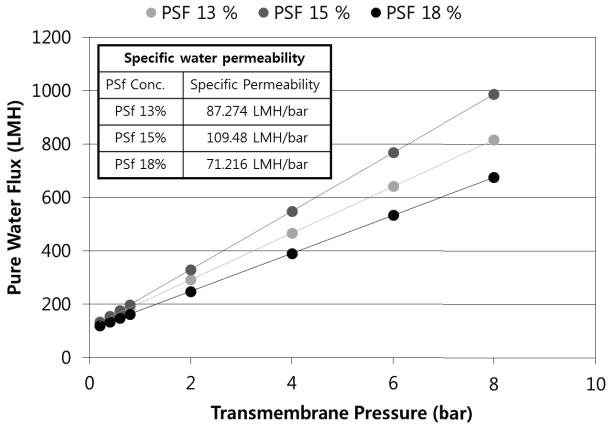

Fig. 4. Pure water permeability (PWP) for PSf support layers with PSf 13%, PSf 15%, and PSf 18% polymer concentration.

(87.274 LMH/bar), and PSf 18 showed the lowest water flux (71.216 LMH/bar). In general, a low polymer concentration induced high water permeability for the asymmetric polymeric membrane due to the presence of more open pores. Despite the larger surface pore size for the PSf 13, the water permeation was higher for the PSf 15 than for the PSf 13. The SEM images for the PSf support layers showed that the PSf 13 polymer matrix was permeated through the PET fabric due to its low viscosity. The PSf polymer blocked the macro spaces in the PET fabric, thereby hindering water permeation and causing a lower pure water flux for the PSf 13 than for the PSf 15. Based on this effect of PSf concentration, PSf 15 was utilized for subsequent TFC FO membrane fabrication because of its characteristics and performance.

3.2. Effect of casting thickness

In the previous section, polymer concentration was confirmed to determine the porous structure of the PSf support layer. The membrane thickness also affected the water permeation flux in the FO mode [1,2], therefore, this was also carefully investigated in this study. In this section, the effect of casting thickness on membrane structure and performance in the FO mode was investigated. The PSf concentration of the polymer solution was fixed at 15 wt% and the solution was casted with different casting thickness of 100, 150, and 200 μm. All the PSf solutions were cast on the PET woven fabric. The PA selective layer was then formed on the PSf support layer surface. Fig. 5 shows the cross-sectional and surface images for the TFC membranes with different casting thicknesses. An asymmetric porous structure was observed for all the membranes, as shown in Figs. 5(a)–(c). The actual thicknesses of PSf support layers are shown in Fig. 6. As the casting thickness increased, the TFC membrane became thicker, which would be expected to decrease the water permeability (actual thickness: 62 μm with a 100 μm casting thickness, 101 μm with a 150 μm casting thickness, 130 μm with a 200 μm casting thickness).

Generally, a thin membrane allowed high water permeability. However, when the PSf support layer was too thin, the PSf support layer might not have fully covered the standing PET fiber strands, which would hinder IP and reduce the membrane selectivity. The PA layer for all TFC membranes was formed on the surface of PSf support layers with a ridge-and-valley structure as shown in Figs. 5(d)–(i), which indicated that the aqueous MPD solution was well positioned on top of the PSf support layer and PA layer was well formed on the top.

3.3. Forward osmosis membrane performance

The TFC membranes with different casting thicknesses of PSf support layers were operated in a lab-scale FO unit to evaluate the membrane performance. The active layers of the membranes were faced to the feed solution (the active layer-feed solution) using a 1 M NaCl draw solution and DI water feed solution. The water flux, RSF, and membrane selectivity are shown in Fig. 7. The water flux significantly decreased and the RSF slightly decreased with increase in casting thickness: the water flux – 15.073 LMH (100 μm), 9.150 LMH (150 μm), and 6.604 LMH (200 μm), while the RSF was 4.393 gMH (100 μm), 3.083 gMH (150 μm), and 2.908 gMH (200 μm). The membrane selectivity increased with increasing casting thickness, with membrane selectivity of 0.3280 g/L (100 μm), 0.3370 g/L (150 μm), and 0.4403 g/L (200 μm). Therefore, the synthetic TFC membrane showed a relatively greater increase in permeability than in salt ion selectivity.

Since all the TFC membranes were fabricated using the same materials and methods, the chemical properties of the membranes, such as hydrophilicity and surface negativity, were not changed. Therefore, the membrane performance was governed by the physical properties of the support layer, such as the membrane porosity and thickness. The effect of the support layer physical properties on the ICP is especially critical when investigating the correlation between the support layer structure and FO performance. The resistance to solute diffusion within the membrane porous support layer (K) was defined as:

$$K = \frac{t\tau}{\varepsilon D_S}$$

where t, τ, ε, and D_S are the membrane thickness, tortuosity, porosity, and the diffusion coefficient of the solute,

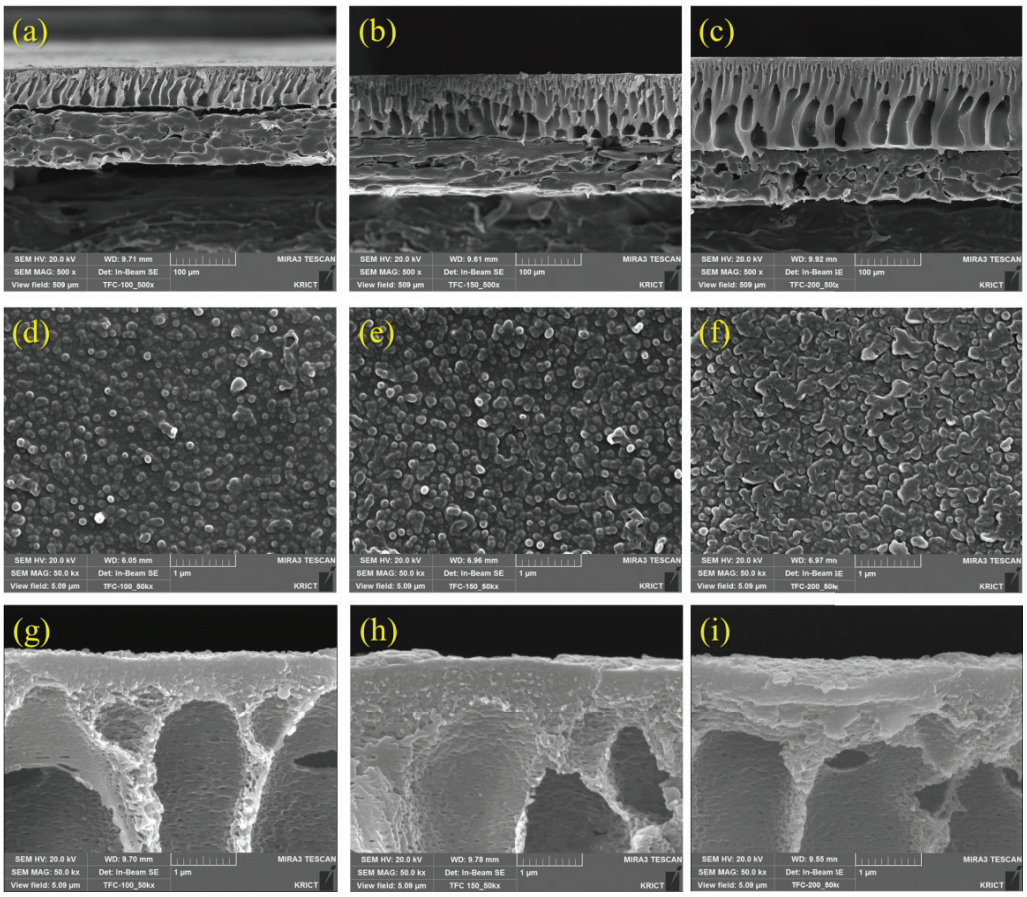

Fig. 5. Scanning electron microscopy (SEM) images of cross-sections and surfaces of thin-film composite (TFC) membranes with different casting thickness: 100 μm (a), (d), and (g); 150 μm (b), (e), and (h); and 200 μm (c), (f), and (i).

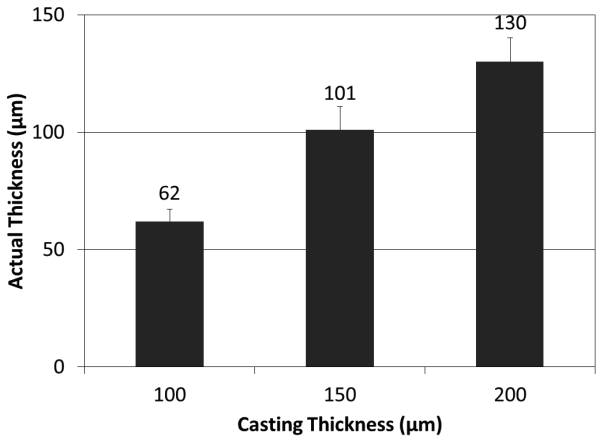

Fig. 6. Actual thickness of thin-film composite (TFC) membranes with different casting thicknesses of PSf support layers.

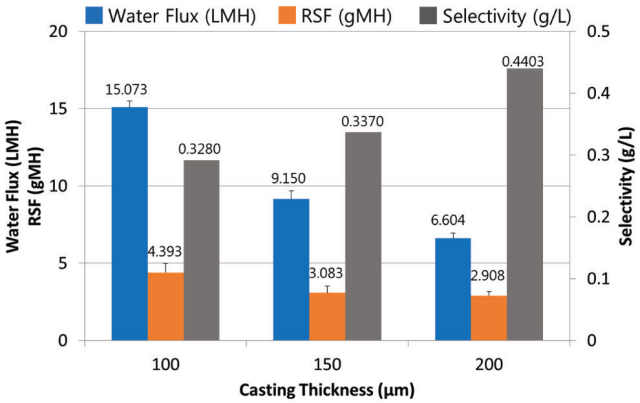

Fig. 7. Forward osmosis (FO) performance under the active layer-feed solution (AL-FS) mode for a thin-film composite (TFC) membrane.

respectively [1]. As discussed above, the membrane porosity was related to the polymer concentration, and the PSf 15 was chosen as an optimized support layer membrane. In this TFC membrane synthesis, the membrane thickness increased as the casting thickness increased. This change in porosity and thickness increased the value of *K*.

Previous studies developed a general governing equation that demonstrated an inverse correlation between the water flux and the *K* value [32,33]. Other recent studies also reported that the ICP caused declines in the water flux [15,33]. Therefore, the changing trends in the water flux and RSF for the synthesized TFC membranes occurred due to the ICP and the changes in the membrane thickness. Based on

this study, TFC membrane prepared by PSf 15 as a support layer with casting thickness of 100 μm (actual thickness: 62 μm) could be proposed as an optimized TFC membrane for FO applications.

4. Conclusion

The effect of fabrication parameters was investigated for the performance of PSf support layers and TFC membranes operated in the FO mode. The following conclusions can be drawn based on the results of this study:

- The PSf polymer concentration in the dope solution and the casting thickness for the PSf support layer were critical factors. These influenced the support layer structure and the resulting membrane performance in the FO mode.
- A 15 wt% concentration of PSf polymer and 100 μm casting thickness were determined as optimal for preparation of a PSf support layer for TFC FO membrane fabrication.
- The results of this study could be utilized for the basic fabrication of a commercial TFC FO membrane. However, other studies of critical fabrication factors are also necessary.

Acknowledgment

This study was supported by the National Research Foundation of Korea (NRF) grant funded by the Korean government (MEST) (No. KK1702-B40). The authors acknowledge Mi-Young Lee in the KAIST "Sustainable Water Environment and Energy Technology Laboratory" for her contributions in the PEG concentration measurements for the MWCO tests.

References

[1] T.Y. Cath, A.E. Childress, M. Elimelech, Forward osmosis: principles, applications, and recent developments, J. Membr. Sci., 281 (2006) 70–87.
[2] S. Zhao, L. Zou, C.Y. Tang, D. Mulcahy, Recent developments in forward osmosis: opportunities and challenges, J. Membr. Sci., 396 (2012) 1–21.
[3] J.R. McCutcheon, R.L. McGinnis, M. Elimelech, A novel ammonia—carbon dioxide forward (direct) osmosis desalination process, Desalination, 174 (2005) 1–11.
[4] J. Herron, Asymmetric Forward Osmosis Membranes, Hydration Technologies Inc., USA, 2006.
[5] J. Wright, R. Johnson, S. Yum, DUROS® osmotic pharmaceutical systems for parenteral and site-directed therapy, Drug Delivery Technol., 3 (2003) 64–73.
[6] L. Chekli, S. Phuntsho, H.K. Shon, S. Vigneswaran, J. Kandasamy, A. Chanan, A review of draw solutes in forward osmosis process and their use in modern applications, Desal. Wat. Treat., 43 (2012) 167–184.
[7] S. Phuntsho, H.K. Shon, S. Hong, S. Lee, S. Vigneswaran, A novel low energy fertilizer driven forward osmosis desalination for direct fertigation: evaluating the performance of fertilizer draw solutions, J. Membr. Sci., 375 (2011) 172–181.
[8] A. Achilli, T.Y. Cath, A.E. Childress, Selection of inorganic-based draw solutions for forward osmosis applications, J. Membr. Sci., 364 (2010) 233–241.
[9] C. Tan, H. Ng, A novel hybrid forward osmosis-nanofiltration (FO-NF) process for seawater desalination: draw solution selection and system configuration, Desal. Wat. Treat., 13 (2010) 356–361.
[10] H.Y. Ng, W. Tang, Forward (direct) osmosis: a novel and prospective process for brine control, Proc. Water Environ. Fed., 2006 (2006) 4345–4352.
[11] K.B. Petrotos, P. Quantick, H. Petropakis, A study of the direct osmotic concentration of tomato juice in tubular membrane–module configuration. I. The effect of certain basic process parameters on the process performance, J. Membr. Sci., 150 (1998) 99–110.
[12] R.E. Kravath, J.A. Davis, Desalination of sea water by direct osmosis, Desalination, 16 (1975) 151–155.
[13] P. McCormick, J. Pellegrino, F. Mantovani, G. Sarti, Water, salt, and ethanol diffusion through membranes for water recovery by forward (direct) osmosis processes, J. Membr. Sci., 325 (2008) 467–478.
[14] S. Adham, J. Oppenheimer, L. Liu, M. Kumar, Dewatering Reverse Osmosis Concentrate from Water Reuse Applications Using Forward Osmosis, Water Reuse Foundation, Alexandria, 2007.
[15] J.R. McCutcheon, R.L. McGinnis, M. Elimelech, Desalination by ammonia–carbon dioxide forward osmosis: influence of draw and feed solution concentrations on process performance, J. Membr. Sci., 278 (2006) 114–123.
[16] T.Y. Cath, N.T. Hancock, C.D. Lundin, C. Hoppe-Jones, J.E. Drewes, A multi-barrier osmotic dilution process for simultaneous desalination and purification of impaired water, J. Membr. Sci., 362 (2010) 417–426.
[17] M.M. Ling, T.-S. Chung, Desalination process using super hydrophilic nanoparticles via forward osmosis integrated with ultrafiltration regeneration, Desalination, 278 (2011) 194–202.
[18] S. Loeb, S. Sourirajan, Sea Water Demineralization by Means of an Osmotic Membrane, Saline Water Conversion—II, American Chemical Society, 1963, pp. 117–132.
[19] I. Alsvik, M.-B. Hägg, Pressure retarded osmosis and forward osmosis membranes: materials and methods, Polymers, 5 (2013) 303.
[20] J.R. McCutcheon, M. Elimelech, Influence of membrane support layer hydrophobicity on water flux in osmotically driven membrane processes, J. Membr. Sci., 318 (2008) 458–466.
[21] N.Y. Yip, A. Tiraferri, W.A. Phillip, J.D. Schiffman, M. Elimelech, High performance thin-film composite forward osmosis membrane, Environ. Sci. Technol., 44 (2010) 3812–3818.
[22] P.W. Morgan, S.L. Kwolek, Interfacial polycondensation. II. Fundamentals of polymer formation at liquid interfaces, J. Polym. Sci., 40 (1959) 299–327.
[23] B. Khorshidi, T. Thundat, B.A. Fleck, M. Sadrzadeh, A novel approach toward fabrication of high performance thin film composite polyamide membranes, Sci. Rep., 6 (2016) 1–10.
[24] H.B. Park, J. Kamcev, L.M. Robeson, M. Elimelech, B.D. Freeman, Maximizing the right stuff: the trade-off between membrane permeability and selectivity, Science, 356 (2017) 1–10.
[25] H.-g. Choi, M. Son, H. Choi, Integrating seawater desalination and wastewater reclamation forward osmosis process using thin-film composite mixed matrix membrane with functionalized carbon nanotube blended polyethersulfone support layer, Chemosphere, 185 (2017) 1181–1188.
[26] P. Li, Effect of polymer dope concentration on the morphology and performance of PES/PDMS hollow fiber composite membrane for gas separation, J. Mater. Sci., 1 (2017) 1–4.
[27] C.A. Smolders, A.J. Reuvers, R.M. Boom, I.M. Wienk, Microstructures in phase-inversion membranes. Part 1. Formation of macrovoids, J. Membr. Sci., 73 (1992) 259–275.
[28] A. Tiraferri, N.Y. Yip, W.A. Phillip, J.D. Schiffman, M. Elimelech, Relating performance of thin-film composite forward osmosis membranes to support layer formation and structure, J. Membr. Sci., 367 (2011) 340–352.
[29] M. Mulder, Basic Principles of Membrane Technology, 2nd ed., Kluwer Academic Publishers, The Netherlands, 1997.
[30] M. Dalwani, N.E. Benes, G. Bargeman, D. Stamatialis, M. Wessling, A method for characterizing membranes during nanofiltration at extreme pH, J. Membr. Sci., 363 (2010) 188–194.
[31] A.F.v. Recum, Handbook of Biomaterials Evaluation: Scientific, Technical and Clinical Testing of Implant Materials, 2nd ed., CRC Press, Philadelphia, 1998.
[32] S. Loeb, L. Titelman, E. Korngold, J. Freiman, Effect of porous support fabric on osmosis through a Loeb-Sourirajan type asymmetric membrane, J. Membr. Sci., 129 (1997) 243–249.
[33] G.T. Gray, J.R. McCutcheon, M. Elimelech, Internal concentration polarization in forward osmosis: role of membrane orientation, Desalination, 197 (2006) 1–8.